Coupling between molecular rotations and OH***O motions in liquid water: Theory and experiment

Guilhem Gallot, S. Bratos, S. Pommeret, Noëlle Lascoux, J.-Cl. Leicknam, M. Kozinski, W. Amir, Geoffrey Gale

Coupling between molecular rotations and OH···O motions in liquid water: Theory and experiment

G. Gallot
Laboratoire d'Optique et Biosciences, École Polytechnique, Route de Saclay, 91128 Palaiseau Cedex, France

S. Bratos
Laboratoire de Physique Théorique des Liquides, Université Pierre et Marie Curie, 4 Place Jussieu, 75252 Paris Cedex 05, France

S. Pommeret
CEA/Saclay, DSM/DRECAM/SCM/URA 331 CNRS, 91191 Gif-sur-Yvette, France

N. Lascoux
Laboratoire d'Optique et Biosciences, École Polytechnique, Route de Saclay, 91128 Palaiseau Cedex, France

J-Cl. Leicknam and M. Koziński
Laboratoire de Physique Théorique des Liquides, Université Pierre et Marie Curie, 4 Place Jussieu, 75252 Paris Cedex 05, France

W. Amir and G. M. Gale
Laboratoire d'Optique et Biosciences, École Polytechnique, Route de Saclay, 91128 Palaiseau Cedex, France

(Received 19 July 2002; accepted 25 September 2002)

A new theory is proposed to describe spectral effects of the coupling between molecular rotations and OH···O motions in liquid water. The correlation function approach is employed together with a special type of development in which the coupling energy of these two motions is the expansion parameter. The isotropy of the liquid medium plays an essential role in this study. Based on this theory, a new infrared pump–probe experiment is described permitting a visualization of molecular rotations at subpicosecond time scales. Full curves relating the mean squared rotational angle and time, and not only the rotational relaxation time, are measured by this experiment. However, very short times where the incident pulses overlap must be avoided in this analysis. The lifetime of OH···O bonds in water is rotation–limited. © *2002 American Institute of Physics.*
[DOI: 10.1063/1.1522378]

I. INTRODUCTION

The past decade has contributed much new information about short time hydrogen bond dynamics in liquid water. This is due to the development of new powerful lasers, generating pico- and femto-second pulses in the mid-infrared spectral region. It now became possible to study this liquid, so essential for the life on our planet, on tiny time scales extending from a few hundreds of femto-seconds to a few tens of pico-seconds. Employing pump–probe techniques, the OH···O motions in liquid water were studied in real time;[1,2] the procedure was similar to that employed by Zewail *et al.* in their breakthrough work on the ICN dissociation.[3,4] No oscillations of the hydrogen bond were detected. Moreover, the coupling between molecular rotations and OH···O motions in water was examined on the same time scales.[5–7] The forces hindering them depend on the distance between the two oxygen atoms, which introduces a correlation between these degrees of freedom. From the other side, physico–chemical properties of various short lived structures present in liquid water were studied too: the hydrogen bond network generates irregularly fluctuating tetrahedral assemblies around each water molecule.[8–10] Finally, recent photon echo experiments brought out unexpectedly fast dynamics of the OH···O grouping, not yet seen before.[11] Femtochemistry of water thus remains a very active branch of science.

The purpose of the present paper is to pursue this effort by describing a new statistical theory of couplings between molecular rotations and the OH···O motions. The correlation function approach is employed all along as well as a special type of expansion in which the energy of coupling between rotational and OH···O motions is the expansion parameter. The isotropy of the liquid system plays a crucial role. Based on theoretical results, a new pump–probe experiment is proposed permitting to visualize HDO rotations in HDO/D_2O solutions in real time. Full curves relating mean squared rotational angles and times, and not only the rotational relaxation time, are measured. However, the overlap of incident pulses at short times severely complicates the analysis. The lifetime of the OH···O bonds in water is shown to be rotation limited.

II. GENERALITIES

Femtosecond dynamics of OH···O bonds in water are most often studied by using ultrafast pump–probe techniques.[1,2] The procedure is based on a well-known relation-

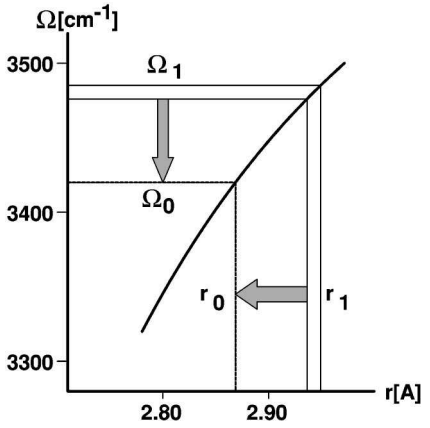

FIG. 1. Relation between the OH···O hydrogen bond length r and the OH link frequency Ω. r_0 and Ω_0 designate the equilibrium values of r and Ω.

ship linking the hydrogen stretching frequency Ω of an OH···O bond and its length r. The stronger the hydrogen bond, the softer the OH link and the lower is its frequency Ω. Following the initial proposal of Rundle and Parasol, a number of empirical relationships were published; the one adopted here is the recent relationship due to Mikenda[12] illustrated in Fig. 1. The experiment then goes as follows. An ultrafast pump pulse of frequency Ω_1, belonging to the conventional OH stretching band of HDO, is used to excite OH vibrations; this excitation results in selecting OH···O bonds of a given length r_1. However, the system does not conserve this nonequilibrium geometry, but returns progressively to the equilibrium; the OH···O bond length then passes from its initial value r_1 to the equilibrium value r_0. Simultaneously, the OH band shifts from the pump frequency Ω_1 to its equilibrium frequency Ω_0. Thus, probing the position of the OH band as a function of the pump–probe delay τ and using the Mikenda relation, the value of the OH···O bond length can be deduced in each moment. It is thus possible to follow its temporal variations directly.

The above experiment was also adapted to the study of HDO rotations in liquid HDO/D_2O solutions.[5–7] The method consists in selecting hydrogen bonds of a specified length r_1 by pumping the system with an appropriate frequency Ω_1. Molecular rotations of the subset of hydrogen bonds created in this way are analyzed next by measuring the rotational anisotropy $R=(S_{\parallel}-S_{\perp})/(S_{\parallel}+2S_{\perp})$ of the system for different probe frequencies Ω_2 and for different time delays τ; the signals $S_{\parallel}$ and $S_{\perp}$ correspond to the parallel and perpendicular electric field configurations, respectively. This quantity is an important indicator of molecular rotations in liquid systems.[13–15] In fact, if (i) the couplings between molecular rotations and other degrees of freedom are absent, and (ii) the time delay τ between the pump and probe pulses are long enough to avoid their overlap, then in very general conditions[16,17]

$$R(\tau)=(2/5)\langle P_2(\cos(\theta(\tau)))\rangle=(2/5)\exp(-3/2\langle\theta^2(\tau)\rangle), \quad (1)$$

where P_2 is the second-order Legendre polynomial and $\theta(\tau)$ the angle between the transition moment vectors in times 0 and τ. Measuring $R(\tau)$ as a function of time τ thus provides the square averaged rotation angle $\langle\theta(\tau)^2\rangle$; this experiment has the intrinsic power of visualizing molecular rotations. The above relation simplifies for times τ long as compared to the correlation time of the molecular angular velocity $\omega=d\theta/d\tau$. Molecular rotations then transform into rotational diffusion, and Eq. (1) takes the well known form $R(\tau)=(2/5)\exp(-\tau/\tau_O)$ where τ_O is the rotational relaxation time. Measuring $R(\tau)$ as a function of τ in these conditions then provides τ_O, but not the full curve $\langle\theta(\tau)^2\rangle$. Finally, it should be stressed that this theory predicts $R(\tau)$ to be independent of Ω_1 and Ω_2.

However, all these conclusions only apply if the conditions (i), (ii) underlying the derivation of Eq. (1) hold true. Are they satisfied in the case of water? The condition (ii) certainly fails at small τ's where the pump and probe pulses overlap, whatever the material under consideration. Unfortunately, the condition (i) is not satisfied neither for water, although the coupling between molecular rotations and remaining degrees of freedom may be absent in other liquids. In fact, $R(\tau)$ was measured as a function of Ω_1 and Ω_2; it was found to be distinctly Ω_1, Ω_2 dependent, which proves the presence of couplings. How to proceed in these conditions? Can Eq. (1) still be applied in spite of this difficulty? A possible, although approximate, way out is to maintain the expression $R(\tau)=(2/5)\exp(-\tau/\tau_O)$ and to consider τ_O, or equivalently the rotational diffusion constant D_R, to depend on the OH···O distance; $R(\tau)$ then becomes in fact frequency dependent. However, introducing a model of this type, does not exempt one of the necessity to construct a fully statistical theory of couplings between molecular rotations and OH···O motions. The purpose of this paper is to present a theory of this kind.

III. THEORY

A. Basic formulas

The system under consideration is a diluted isotopic solution HDO/D_2O in thermal equilibrium. It contains N solute molecules in a volume V. A pump pulse of frequency Ω_1 brings the system in an excited state; and a probe pulse of frequency Ω_2 explores its return in its ground state at time τ. The pump and probe electric fields are $\mathbf{E}_1=(E_{1x},E_{1y},E_{1z})$ and $\mathbf{E}_2=(E_{2x},E_{2y},E_{2z})$, and the total electric field is $\mathbf{E}=(E_{1x}+E_{2x},E_{1y}+E_{2y},E_{1z}+E_{2z})$. These two fields are not parallel to each other in general.

The quantity measured experimentally is the pump–probe signal $S(\Omega_1,\Omega_2,\tau)$. It is defined as the total probe absorption $W(\Omega_1,\Omega_2,\tau)$ in presence of the pump minus the probe absorption $W(\Omega_2)$ in absence of the pump. Then, if $\mathbf{M}(M_x,M_y,M_z)$ denotes the electric dipole moment of the system, the following formula applies:[18,19]

$$\begin{aligned}S(\Omega_1,\Omega_2,\tau)=(2/\hbar^3)Im\int_{-\infty}^{\infty}\int_0^{\infty}\int_0^{\infty}\int_0^{\infty}dt\ d\tau_1\ d\tau_2\ d\tau_3\\ \times\langle\dot{E}_{2i}(\mathbf{r},t)E_j(\mathbf{r},t-\tau_3)\\ \times E_k(\mathbf{r},t-\tau_3-\tau_2)E_l(\mathbf{r},t-\tau_3-\tau_2-\tau_1)\rangle_E\\ \times\langle M_l(0)[M_k(\tau_1),[M_j(\tau_1+\tau_2),\\ \times M_i(\tau_1+\tau_2+\tau_3)]]\rangle_S. \quad (2)\end{aligned}$$

This expression involves two kinds of 4-time correlation functions: the correlation functions of the total and the probe electric fields $\mathbf{E}(\mathbf{r},t)$ and $\mathbf{E}_2(\mathbf{r},t)$ and those of the electric dipole moment $\mathbf{M}(t)$ of the system. The indices i, j, k, l denote the Cartesian components of these vectors; the Einstein convention is employed all along indicating a summation over doubled indices. The average $\langle\ \rangle_S$ is over states of the nonperturbed liquid system, and the average $\langle\ \rangle_E$ is over all possible realizations of the incident electric fields. The symbol [,] denotes a commutator and the dot a time derivative. Choosing the electric fields $\mathbf{E}_1$, $\mathbf{E}_2$ of appropriate form, all possible cases of polarization may be treated. It should be noted that Eq. (2) represents an exact third-order perturbation theory result.

B. Model

The above equation will now be employed to study rotational anisotropy of an isotopic water solution. The pump electric field $\mathbf{E}_1(\mathbf{r},t)=(0,0,E_{\text{pump}}(\mathbf{r},t))$ is supposed to be polarized along the laboratory fixed z axis, and the probe electric field to be either $\mathbf{E}_2(\mathbf{r},t)=(0,0,E_{\text{probe}}(\mathbf{r},t))$ in the parallel electric field configuration or $\mathbf{E}_2(\mathbf{r},t)=(0,E_{\text{probe}}(\mathbf{r},t),0)$ in the perpendicular electric field configuration. The total electric field is then $\mathbf{E}(\mathbf{r},t)=(0,0,E_{\text{pump}}(\mathbf{r},t)+E_{\text{probe}}(\mathbf{r},t))$ in the first case, and $\mathbf{E}(\mathbf{r},t)=(0,E_{\text{probe}}(\mathbf{r},t),E_{\text{pump}}(\mathbf{r},t))$ in the second. In all circumstances one has $E_{\text{probe}}\ll E_{\text{pump}}$.

Unfortunately, Eq. (2) cannot be applied to the present case without approximations, and a model must be used; it involves the following assumptions: (i) The OH vibrator of HDO/D_2O is assimilated to a two-level quantum system, perturbed by random solvent–solute interactions. All remaining degrees of freedom of the system constitute a classical thermic bath. (ii) Time evolution of the dipole moment $\mathbf{M}$ is governed by the modified Heisenberg equation

$$\frac{d}{dt}\mathbf{M}=\frac{i}{\hbar}[H,\mathbf{M}]-\Gamma\mathbf{M}, \tag{3}$$

where H is an adiabatic Hamiltonian and Γ the Pauli relaxation operator. The ith component M_i of $\mathbf{M}$ is written $M_i=Mu_i$, where M is the length of $\mathbf{M}$ and $\mathbf{u}$ its unit vector. The variable M is quantum-mechanical whereas $\mathbf{u}$ is classical. (iii) The pump and probe electric fields have slowly varying Gaussian amplitudes $E_{\text{pump}}(t)$, $E_{\text{probe}}(t)$ and random phases $\phi_{\text{pump}}(t)$, $\phi_{\text{probe}}(t)$, independent of each other

$$\begin{aligned}E_{\text{pump}}(\mathbf{r},t)&=2\ \text{Re}[E_{\text{pump}}(t')\\&\quad\times\exp(i\mathbf{k}_{\text{pump}}\mathbf{r}-i\Omega_{\text{pump}}t')\exp(i\phi_{\text{pump}}(t'))],\\E_{\text{probe}}(\mathbf{r},t)&=2\ \text{Re}[E_{\text{probe}}(t)\\&\quad\times\exp(i\mathbf{k}_{\text{probe}}\mathbf{r}-i\Omega_{\text{probe}}t)\exp(i\phi_{\text{probe}}(t))],\end{aligned} \tag{4}$$

where $t'=t+\tau$. Models of this type are of current use in laser physics. However, it only applies if the $v=0\leftrightarrow v=1$, but not the $v=1\rightarrow v=2$, transition is involved in the experiment; a three-level model would be required otherwise. In practice, this means the excitation be must be confined to the 3500 cm^{-1} spectral region.

The above model still needs to be completed by presenting time scales of the problem. The hydrogen bond dynamics in liquid water are controlled by three relaxation times. The first of them is the life time τ_p of the OH vibrator in its first excited state. It is surprisingly short: according to the most recent determinations it is of the order of 1.0 ps.[1,2,9,10,20] Another characteristic time is the solvent relaxation time τ_Ω: intermolecular forces are feebly modified by vibrational excitation, which leads to a rupture of thermic equilibrium. Experiment and molecular dynamics simulations proposed values of the order of 0.7 ps for it.[1,2,21–25] Finally, the rotational relaxation time τ_O measures the progressive loss of orientational coherence; it corresponds to the correlation time of the second spherical harmonics. Involved in many experimental situations, it has been measured or calculated by a number of authors.[26–31] The values of the order of 2.5 ps may be considered as representative. A last time playing a role in the present context, although only indirectly, is the dephasing time τ_d: this is the time in which the phase coherence of the ν_{OH} vibrations is lost due to the frequency dispersion, and is of the order of 15 fs. It results from the above data that very short laser pulses, not longer than a few hundreds of femtoseconds, are required in this study. For convenience, the paper is written as to permit to skip, at first reading, the technical details which follow and pass to Sec. IV directly.

C. Dipole moment correlation functions

1. Liouville pathways of the system

It is convenient to start this calculation by studying dipole moment correlation functions. As the coupling between rotations and OH···O motions has to be fully accounted for, a considerable effort is required to do it. The calculation involves the following steps. (i) The dipole moment of the system is written $\mathbf{M}=M\,\mathbf{u}$, where M is quantum-mechanical and $\mathbf{u}$ classical. Then:

$$\begin{aligned}&\langle M_l(o)[M_k(\tau_1),[M_j(\tau_1+\tau_2),M_i(\tau_1+\tau_2+\tau_3)]]\rangle_S\\&\quad=\langle u_l(0)u_k(\tau_1)u_j(\tau_1+\tau_2)u_i(\tau_1+\tau_2+\tau_3)\\&\qquad\times M(0)[M(\tau_1),[M(\tau_1+\tau_2),M(\tau_1+\tau_2+\tau_3)]]\rangle_S.\end{aligned} \tag{5}$$

The quantities u_i, u_j, u_k, u_l are Cartesian components of the unit vector $\mathbf{u}$; as they are classical, they may be shifted at will. The operation $\langle\ \rangle_S$ involves the average over the quantum states of the OH vibrator as well as that over the bath degrees of freedom; one has $\langle\ \rangle_S=\langle Tr\rho\ \rangle$, where ρ is the vibrational density matrix and $\langle\ \rangle$ designates the averaging over the bath. (ii) The incident electric fields are polarized either along the z or along the y axis. In these conditions, correlation functions in which the indices i, j, k, l are all equal to z, as well as those in which two indices are equal to y and two to z only survive. This is a consequence of the isotropy of a liquid system. (iii) The above expression for correlation functions can be given a more explicit form by developing it over the quantum states of the OH vibrator. The matrix elements M_{00} and M_{11} do not contribute to the OH band intensity and can safely be neglected. The matrix elements $M_{01}(t)$ and $M_{10}(t)=M_{01}(t)^*$ may be determined by solving Eq. (3), which gives $M(t)_{01}=M_{01}\times\exp[-i\int_0^t dt\ \omega(t)-\Gamma t]$ where $\hbar\omega=H_{11}-H_{00}$. Then, if only the ground vibrational state is thermally occupied, one finds

$$\langle M_l(0)[M_k(\tau_1),[M_j(\tau_1+\tau_2),M_i(\tau_1+\tau_2+\tau_3)]]\rangle_S$$
$$=2(M_{01}M_{10})^2\exp(-3\Gamma\tau_1-2\Gamma\tau_2-\Gamma\tau_3)$$
$$\times\left\{\left\langle u_l(0)u_k(\tau_1)u_j(\tau_1+\tau_2)u_i(\tau_1+\tau_2+\tau_3)\exp\left[i\int_0^{\tau_1}dt\ \omega(t)\right]-i\int_0^{\tau_1+\tau_2}dt\ \omega(t)\right]+i\int_0^{\tau_1+\tau_2+\tau_3}dt\ \omega(t)\right\rangle$$
$$+\left\langle u_l(0)u_k(\tau_1)u_j(\tau_1+\tau_2)u_i(\tau_1+\tau_2+\tau_3)\exp\left[i\int_0^{\tau_1+\tau_2+\tau_3}dt\ \omega(t)-i\int_0^{\tau_1+\tau_2}dt\ \omega(t)+i\int_0^{\tau_1}dt\ \omega(t)\right]\right\rangle$$
$$-\left\langle u_l(0)u_k(\tau_1)u_j(\tau_1+\tau_2)u_i(\tau_1+\tau_2+\tau_3)\exp\left[i\int_0^{\tau_1+\tau_2}dt\ \omega(t)-\int_0^{\tau_1+\tau_2+\tau_3}dt\ \omega(t)+\int_0^{\tau_1}dt\ \omega(t)\right]\right\rangle$$
$$-\left\langle u_l(0)u_k(\tau_1)u_j(\tau_1+\tau_2)u_i(\tau_1+\tau_2+\tau_3)\exp\left[i\int_0^{\tau_1}dt\ \omega(t)-i\int_0^{\tau_1+\tau_2+\tau_3}dt\ \omega(t)+i\int_0^{\tau_1+\tau_2}dt\ \omega(t)\right]\right\rangle\right\}. \quad (6)$$

The four terms entering in this expression correspond to four different pathways in the Liouville space of operators.[32]

2. Series expansion for rotation–vibration correlations

Where are the effects of the rotation–vibration correlation hidden? In their absence, the terms of Eq. (6) would all factorize into a rotational and a vibrational correlation function, respectively; this is usually assumed to be legitimate. On the contrary, if the correlation is present, this step is strictly forbidden. A method must then be invented to treat the problem in its increased complexity. The one employed here consists of introducing a particular sort of series expansion, the principle of which is as follows.[33] Let X and Y be two correlated stochastic variables and λ a real number. Moreover, let the average over the stochastic process (X,Y) be designated by $\langle\ \rangle$. Then, using the cumulant expansion theorem and expressing the cumulant average by the symbol $\langle\ \rangle_c$, one can write

$$I(\lambda)=\langle\exp(iX+\lambda Y)\rangle \Rightarrow \left(\frac{dI}{d\lambda}\right)_{\lambda=0}=\langle Y\exp(iX)\rangle,$$
$$I(\lambda)=\exp\left[\langle iX+\lambda Y\rangle_c+\frac{1}{2!}\langle(iX+\lambda Y)^2\rangle_c+\frac{1}{3!}\langle(iX+\lambda Y)^3\rangle_c+\cdots\right]$$
$$\Rightarrow \langle Y\ \exp(iX)\rangle \equiv\left(\frac{dI}{d\lambda}\right)_{\lambda=0}=\left[\langle Y\rangle_c+\ i\langle XY\rangle_c-\frac{1}{2}\langle X^2Y\rangle_c+\cdots\right]\times\langle\exp(iX)\rangle. \quad (7)$$

This is the series expansion which was desired. Its leading term $\langle Y\rangle\ \langle\exp(iX)\rangle$ expresses the average $\langle Y\ \exp(iX)\rangle$ in absence of correlation; and its higher order terms $i\langle XY\rangle_c\langle\exp(iX)\rangle, -1/2\langle X^2Y\rangle_c\langle\exp(iX)\rangle$, etc., describe the correlation effects. The stronger the correlation, the slower is the convergence. On the contrary, only the zero and first order terms need to be considered if it is weak. This last condition will be taken as granted in what follows.

The above technique will now be applied in the present study. In fact, the terms in curly brackets of Eq. (6) can all be given the form $\langle Y\exp(iX)\rangle$ by simply choosing the variables X,Y properly. It suffices to take $X=\int_0^{\tau_1}dt\ \omega(t)-\int_0^{\tau_1+\tau_2}dt\ \omega(t)+\int_0^{\tau_1+\tau_2+\tau_3}dt\ \omega(t)$ and $Y=u_l(0)u_k(\tau_1)u_j(\tau_1+\tau_2)u_i(\tau_1+\tau_2+\tau_3)$ in its first term, and to proceed similarly in the three others. The problem then reduces to that of determining the averages $\langle Y\rangle_c$, $\langle XY\rangle_c$, $\langle\exp(iX)\rangle$ for each possible choice of X,Y, i.e., for each Liouville pathway of the system. Detailed calculations are given below.

3. Details of calculations

One starts by calculating the quantities $\langle\exp(iX)\rangle$. They represent vibrational 4-time correlations functions in absence of rotation–vibration coupling. Occurring frequently in various domains of nonlinear spectroscopy, these functions are well known; see, e.g., Refs. 32 and 34. The cumulant expansion theorem leads to the following result:

$$\langle\exp(iX)\rangle=e^{i\omega_0(\tau_1\pm\tau_3)}\exp\left[-\frac{1}{2}\int_0^{\tau_1}\int_0^{\tau_1}dt\ dt'\beta(t,t')-\frac{1}{2}\int_0^{\tau_3}\int_0^{\tau_3}dt\ dt'\beta(t,t')\pm\int_0^{\tau_1}\int_0^{\tau_3}dt\ dt'\beta(t+\tau_1+\tau_2,t')\right], \quad (8)$$

where $\omega_0=\langle\omega\rangle$ is the mean frequency of the transition $v=1\rightarrow v=0$ in solution, and $\beta(t,t')=\langle\omega(t)\omega(t')\rangle_c$ is the frequency shift correlation function; in what follows, it will be given a simple exponential form $\beta(\tau)=\langle\omega^2\rangle_c\times\exp(-\pi/\tau_\Omega)$. The signs $\pm$ depend on the Liouville pathway which was chosen. Vibrational correlation functions vanish for τ_1,τ_3 large as compared to τ_d and τ_Ω. These variables are thus limited which is important for subsequent developments of the theory.

The quantities $\langle Y\rangle_c$ are studied next. They correspond to various rotational 4-time correlation functions in absence of

rotation–vibration coupling. For example, $\langle Y\rangle_c$ is equal to $\langle u_z(0)u_z(\tau_1)u_z(\tau_1+\tau_2)u_z(\tau_1+\tau_2+\tau_3)\rangle$ in the parallel electric field configuration, whatever the Liouville pathway; this simplicity is lost in the perpendicular electric field configuration. The dependence of these functions on τ_1, τ_3 can safely be suppressed: these variables are limited by the times τ_d, τ_Ω, which in their turn are small compared to the rotational relaxation time τ_O. The resulting 2-time correlation functions may be calculated by assuming that dynamic variables $u_l u_k - \langle u_l u_k\rangle$, etc., obey the simple Langevin equation of motion. Proceeding in this way one finds

$$\begin{aligned}
&\langle u_z(0)u_z(0)u_z(\tau_2)u_z(\tau_2)\rangle = \tfrac{1}{9}(1+\tfrac{4}{5}e^{-\zeta\tau_2}) \quad (\parallel),\\
&\langle u_z(0)u_z(0)u_y(\tau_2)u_y(\tau_2)\rangle = \tfrac{1}{9}(1-\tfrac{2}{5}e^{-\zeta\tau_2}) \quad (\perp),\\
&\langle u_z(0)u_y(0)u_z(\tau_2)u_y(\tau)\rangle = \tfrac{1}{15}e^{-\zeta\tau_2} \quad (\perp),
\end{aligned} \tag{9}$$

where $\zeta = 1/\tau_O$. The first of these three rotational correlation functions occurs in problems in which the pump and probe electric fields are parallel to each other, and the latter two are present in those in which the two fields are perpendicular.

Finally, the quantities $\langle XY\rangle_c$ still remain to be treated. As they express rotational–vibrational coupling effects, they are central objects of the present theory. Their form varies when going from one Liouville pathway to another, but their general aspect is always the same,

$$\begin{aligned}
\langle XY\rangle_c = \pm i\int_0^{\tau_1} dt' \langle u_l(0)u_k(\tau_1)u_j(\tau_1+\tau_2)\\
\times u_i(\tau_1+\tau_2+\tau_3)\Delta\omega(t')\rangle\\
+ i\int_0^{\tau_3} dt' \langle u_l(0)u_k(\tau_1)u_j(\tau_1+\tau_2)\\
\times u_i(\tau_1+\tau_2+\tau_3)\Delta\omega(t'+\tau_1+\tau_2)\rangle,
\end{aligned} \tag{10}$$

where $\Delta\omega(t) = \omega(t) - \langle\omega\rangle$. Detailed calculations involve the following steps. (i) The variables τ_1, τ_3, and t' entering into the 5-time correlation functions of Eq. (10) are limited by the times τ_d, τ_Ω. From the other side, the correlation times associated with them are expected to be of the order of, or only slightly smaller than τ_O. Then, as τ_d, τ_Ω are small as compared to τ_O, the dependence on τ_1, τ_3, and t' may be suppressed in all integrands, and the 5-time correlation functions become simple 2-time correlation functions. This time scale argument reduces massively the complexity of the problem, and makes calculations practicable. (ii) The variables $u_l u_k - \langle u_l u_k \Delta\omega\rangle$, etc., are supposed to obey the simple Langevin equation of motion, and to decay with the same decay constant ζ'. The quantities $\langle u_z^2\Delta\omega\rangle$, $\langle u_z^4\Delta\omega\rangle$, and $\langle u_z^2 u_y^2\Delta\omega\rangle$ which appear in the calculation can be determined by considering the isotropy of the liquid medium. One finds, for example, $\langle\Delta\omega\rangle = \langle\Delta\omega(u_x^2+u_y^2+u_z^2)\rangle = 0 \Rightarrow \langle\Delta\omega u_z^2\rangle = 0$, etc. Setting $\alpha = \langle u_z^4\Delta\omega\rangle$ there results

$$\begin{aligned}
&\langle XY\rangle_c = -i\alpha(\pm\tau_1+\tau_3)\exp(-2\zeta'\tau_2) \quad (\parallel),\\
&\langle XY\rangle_c = \tfrac{1}{2}i\alpha(\pm\tau_1+\tau_3)\exp(-2\zeta'\tau_2) \quad (\perp).
\end{aligned} \tag{11}$$

The upper of the above two expressions for $\langle XY\rangle_c$ is valid if the electric fields $\mathbf{E}_1, \mathbf{E}_2$ are parallel to each other, and the lower if they are perpendicular. From the other side, the signs $\pm$ refer to different Liouville pathways of the system, i.e., to different terms in curly brackets of Eq. (6). Rotation–vibration coupling effects thus depend on the 2-time correlation function $\langle u_z^2(0)u_z^2(\tau_2)\Delta\omega(\tau_2)\rangle = \alpha\exp(-2\zeta_2'\tau_2)$ and vanish at times τ_2 such that $\tau_2 \gg 1/\zeta'$. The quantity α can thus be interpreted as a rotation–vibration coupling constant. Astonishingly enough, in spite of its complexity the present analysis leads to comparatively simple, although nontrivial, results. Treating this complexity–simplicity is entirely submitted to the isotropy of liquid medium.

The final expressions for dipole moment correlation functions may be obtained by collecting the above results for $\langle\exp(iX)\rangle$, $\langle Y\rangle_c$, and $\langle XY\rangle_c$. The sums $(\langle Y\rangle_c + \langle XY\rangle_c)\exp(iX)$ have to be evaluated for all possible Liouville pathways, i.e., for each of the four terms of Eq. (6). As stated earlier, the dipole moment correlation functions required for determination of rotational anisotropy in present conditions are those which correspond to the indices $zzzz$, $zzyy$, $zyzy$, and $zyyz$; other combinations of indices i,j,k,l are irrelevant for the present problem. This ends the study of dipole moment correlation functions in the presence of rotational–vibrational couplings.

D. Electric field correlation functions

The calculation of these functions is based on the fact that the wavelength λ of the optical radiation is much longer than molecular dimensions, but much smaller than experimental cell dimensions. However, molecular motions are probed over distances $l \ll \lambda$. A system experiencing a spatially varying electric field is then dynamically equivalent to an ensemble of subsystems submitted to a spatially constant electric field, but different when going from one subsystem to another. The vector $\mathbf{r}$ in $\mathbf{E}_1(\mathbf{r},t)$, $\mathbf{E}_2(\mathbf{r},t)$ no longer denotes a space point, but selects a given subsystem. It is thus legitimate to work with a spatially constant electric fields and to average the results over $\mathbf{r}$ at the end of the calculation. If the incident electric fields are coherent, the electric field correlation function takes its simplest possible form. Recalling that in the parallel electric field configuration the pump and probe electric fields are $\mathbf{E}_1(\mathbf{r},t) = (0,0,E_{\text{pump}}(\mathbf{r},t))$ and $\mathbf{E}_2(\mathbf{r},t) = (0,0,E_{\text{probe}}(\mathbf{r},t))$, whereas in the perpendicular electric field configuration they are $\mathbf{E}_1(\mathbf{r},t) = (0,0,E_{\text{pump}}(\mathbf{r},t))$ and $\mathbf{E}_2 = (0,E_{\text{probe}}(\mathbf{r},t),0)$, one finds

$$\begin{aligned}
&\langle \dot{E}_{2i}(\mathbf{r},t)E_j(\mathbf{r},t-\tau_3)E_k(\mathbf{r},t-\tau_3-\tau_2)E_l(\mathbf{r},t-\tau_3-\tau_2-\tau_1)\rangle\\
&= \sum_s\sum_t\sum_u C_{stu}E^*_{\text{probe}}(t)E_{\text{probe}}(t_s)E^*_{\text{pump}}(\tau+t_t)\\
&\quad\times E_{\text{pump}}(\tau+t_u)\exp(i\Omega_{\text{probe}}(t-t_s)+i\Omega_{\text{pump}}(t_t-t_u)),
\end{aligned} \tag{12}$$

where $t_1 = \tau_3$, $t_2 = t-\tau_3-\tau_2$, $t_3 = t-\tau_3-\tau_2-\tau_3$ and C_{stu} are constant coefficients; the indices $s \neq t \neq u$ run from 1 to 3. These coefficients C_{stu} depend on the choice of i, j, k, l. They are thus different according to whether the function

under consideration is $\langle E_z E_z E_z E_z \rangle$, $\langle E_y E_y E_z E_z \rangle$, $\langle E_y E_z E_y E_z \rangle$, and $\langle E_y E_z E_z E_y \rangle$. As stated earlier, Eq. (12) only applies if the laser fields are coherent. If they are not, the quantity between the square brackets must still be averaged over the random processes which are at the origin of the incoherence. The results depend on the physical nature of this latter process. This ends the study of 4-time electric field correlation functions; for a more detailed discussion, see the review in Ref. 18.

E. Numerical integrations

Before starting numerical work, various numerical data must still be fixed. Different relaxation times entering into the definition of dipole moment correlation functions were taken, whenever possible, from the published computer simulation work. This is true for the solvent relaxation time τ_Ω and the rotational relaxation time τ_O. The value of 0.7 ps was adopted for the former as suggested by Diraison *et al.*;[22] and the value of 2.5 ps was ascribed to the latter, following Impey *et al.* as well as many others.[27] Unfortunately, this purely theoretical attitude could not be maintained up to the end. Computer simulated population relaxation times τ_p are not accurate enough and the constants α, ζ' were never calculated. τ_p was thus transferred from our previous experiments[1,2] where it was given the value of 1.3 ps, $1/\zeta'$ was assimilated to τ_O, and a constant α of -0.7 cm^{-1} permitted to fit the experimental data. The duration of the incident pulses was supposed to be 150 fs for both pump and probe; and the phases $\phi_{\text{pump}}(t)$, $\phi_{\text{probe}}(t)$ were assumed to be slowly modulated.

It remains to sketch procedures employed to perform multidimensional integrations over the variables t, τ_1, τ_2, τ_3 involved in Eq. (2) for $S(\Omega_1,\Omega_2,\tau)$. The integration over the variable t appearing only in the field's terms was realized analytically using a symbolic computation software (Maple). The integration over τ_1, τ_2, τ_3 was performed numerically by employing the Romberg integration method, after two changes of variables on each τ_i. Proceeding in this way, an extremely robust and fast integration C++ program was provided from a large number of analytical expressions given by Maple. The time needed to compute a time step on a personal computer was of the order of a second. This method of integration can easily be extended to any nonlinear experiment such as photon echo or transient grating.

IV. THEORETICAL RESULTS

The principal results of the present theory will now be described. The main questions requiring a theoretical interpretation are as follows: Which are spectral effects of correlations between molecular rotations and the OH···O motions in HDO/D_2O solutions? What happens at the very shortest times? Does rotational anisotropy $R(\tau)$ permit a real time visualization of molecular rotations in presence of correlations? A first flavor of what the final answer could be comes from a theory generated result stating that, even if HDO rotations and OH···O motions are correlated, the quantity $S_\parallel + 2S_\perp$ remains independent of rotational dynamics, whereas $S_\parallel - S_\perp$ does depend on it. This can easily be proved by adding in Eq. (11) for $\langle XY \rangle_c$ the first expression and twice the second; this sum vanishes. One concludes that at least some basic properties of $R(\tau)$ survive in presence of correlations. This result is due to the isotropy of the liquid medium, and is by no means model dependent.

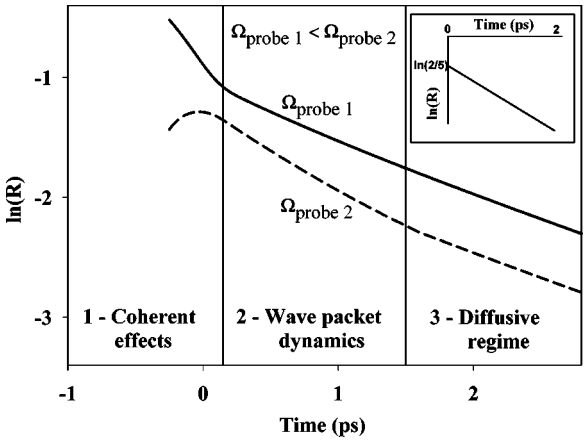

FIG. 2. Schematic presentation of R in presence of rotation–vibration coupling effects. The insert reproduces the results of the simple theory. Coherent effects dominate in the time domain 1, wave packet dynamics governs the time domain 2, whereas rotational diffusion is characteristic of the time domain 3. In this figure $\Omega_{\text{probe 1}}$ and $\Omega_{\text{probe 2}}$ represent two values of the probe frequency Ω_{probe}.

A more complete answer to the above questions is contained in Fig. 2; the insert illustrates the simple theory in absence of correlations. The following comments refer to two-color experiments realized at a fixed Ω_{pump} and variable Ω_{probe}'s. (i) Three time domains have to be distinguished. The first of them corresponds to times $\tau < 200$ fs: the pump and probe pulses overlap, or overlap partially, in this region. The second extends from 200 to 1500 fs, approximately: the pump-generated wave packets are available in a great number, as are the compressed or elongated OH···O bonds. Finally, in the third time domain $\tau > 1500$ fs, the wave packets are destroyed and the statistical equilibrium is reached again. (ii) In the first domain, $\ln(R(\tau))$ deviates from the limiting value of ln(2/5), increasing or decreasing at negative τ's as a function of Ω_{probe}. This seemingly erratic behavior, not yet reported in the literature, is due to the pump–probe coherence and is illustrated in Fig. 3. The dotted curves designate the anisotropy calculated by the complete theory, and the full curves that obtained by neglecting the coherent contributions. The ''anomalous'' behavior of $R(\tau)$ at short τ's disappears in the latter case. (iii) In the second time domain, $\ln(R(\tau))$ measures the square averaged rotation angle $\langle \theta^2(\tau) \rangle$ of the OH link. These rotations cannot be assimilated to a rotational diffusion: the dependence of $\langle \theta^2(\tau) \rangle$ on τ is not linear. Rotational angles $\theta(\tau)$ are smaller for the low than for the high Ω_{probe}'s; this behavior was expected:[5–7] hydrogen bonds ''seen'' are shorter in the former case than in the latter (Fig. 1). (iv) In the third time domain, a family of parallel straight lines with a slope corresponding to $\tau_O = 2.5$ ps is observed. Individual straight lines are shifted vertically with respect to each other, as a function of Ω_{probe}; the straight lines corresponding to small probe frequencies are placed higher than those associated with large ones. This observa-

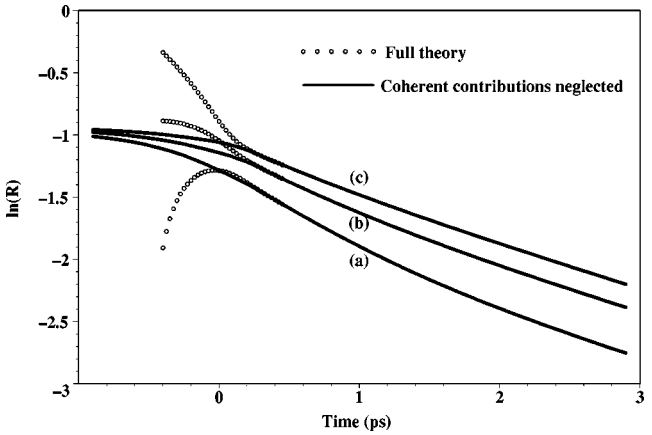

FIG. 3. Rotational anisotropy $R(\tau,\Omega_1,\Omega_2)$calculated by the full theory (dotted curves) and by a theory in which the coherent contributions are suppressed (full curves). The pump frequency Ω_{pump} is equal to 3510 cm^{-1} and Ω_{probe} frequencies are equal to (a) 3510, (b) 3450, and (c) 3410 cm^{-1}, respectively.

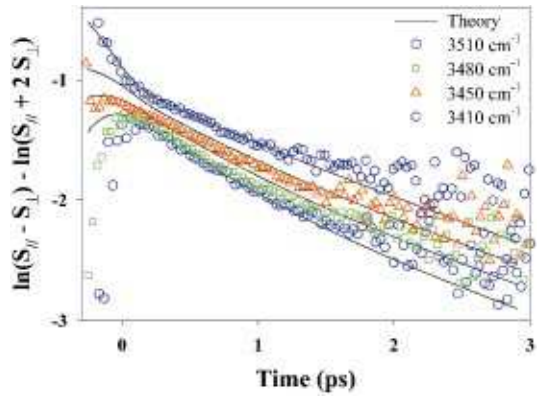

FIG. 4. (Color) Rotational anisotropy R measured experimentally (symbols O, □, △, ◇), and calculated theoretically (full curves). The pump frequency Ω_{pump} is equal to 3510 cm^{-1}, and the probe frequencies Ω_{probe} are equal to 3510, 3480, 3450, and 3410 cm^{-1}, respectively.

tion indicates that in this time period water molecules execute a normal rotational diffusion with a normal relaxation time τ_{O}. However, the short time memory of the system is not entirely lost: molecules having rotated faster in the second time period are deflected more than those which were slower, and the corresponding straight lines lie lower. An approximate analysis permits to guess the size of this effect: if the difference of the probe frequencies is equal to $\Delta\Omega$, the separation of the straight lines is equal to $\Delta(\ln(R)) = (45/4)(\alpha/\beta)(\Delta\Omega)$. The experimentally obtained coupling constant α is negative: the hydrogen bonds shorter than the average of 2.86 A thus contribute more to the coupling constant than the long hydrogen bonds.

In summary, three main effects are predicted by this theory. The first is that correlations between rotations and OH···O motions transform an initially unique curve $R = R(\tau)$ into a family of curves $R = R(\tau,\Omega_{\text{pump}},\Omega_{\text{probe}})$. This effect can be considered as a signature of correlated motions. The second effect is the interference of the pump and probe pulses at short times where they overlap. Rotational anisotropy $R(\tau,\Omega_{\text{pump}},\Omega_{\text{probe}})$ no longer remains a useful indicator of rotational dynamics at these time scales. Finally, if this short time domain is eliminated, rotational anisotropy permits to visualize molecular rotations even if correlations are present. In fact, outside the overlap region, the quantity $\ln R(\tau,\Omega_{\text{pump}},\Omega_{\text{probe}}) - \ln(2/5)$ is still equal to 3/2 times $\langle\theta^2(\tau)\rangle$ at given $\Omega_{\text{pump}},\Omega_{\text{probe}}$. Then using the relation of Fig. 1, the curves just described may be transformed into those relating $\sqrt{\langle\theta^2(\tau)\rangle}$ and τ. A monocolor experiment is required to monitor molecular rotations in hydrogen bonds of a fixed length; a two-color experiment is needed to follow these motions in contracting or expanding hydrogen bonds. One concludes that, if the necessary precautions are taken, ultrafast laser spectroscopy permits to ''film'' molecular rotations in water.

V. VISUALIZING MOLECULAR ROTATIONS IN REAL TIME

In view of the very explicite nature of the above statements, it was decided to check them experimentally. A pump–probe experiment was thus set up having the following characteristics: Its central element was a titanium–sapphire amplifier, delivering 130 fs pulses at 800 nm with a repetition rate of 1 kHz. It drived two lines of pulses, tuned independently in the midinfrared. The principle of the generation was the parametric amplification of a quasicontinuum in the near infrared, followed by a frequency mixing in the midinfrared. The features of the sources were as follows. The more energetic line (the pump) produced pulses having duration of 150 fs and a spectral width of 65 cm^{-1}. It delivered more than 10 μJ between 2800 and 4800 cm^{-1}. The weaker line (the probe) had similar characteristics but with a maximum energy 10 times less. A motorized optical delay line precisely controlled the delay between the pump and the probe. In order to measure the anisotropy, the probe was turned at 45° from the pump by a midinfrared half-wave plate; the state of polarization was controlled by filtration after a Glan–Taylor prism, which compensated for a possible ellipticity of the outgoing beam. The sample was 100 μm thick and contained 1% HDO in D_2O at room temperature; it was circulated to avoid heating problems. It should be stressed that this experiment is intrinsically difficult. The anisotropy R being defined as a ratio of two signals, the error bars become excessive whenever the latter are weak; this is always the case for negative pump–probe delay times as well as for times exceeding 2 ps. Nevertheless, the results are of a good quality in the interval between 0 and 2.5 ps; the accuracy is smaller out of this interval.

The anisotropy curves obtained with excitation at 3510 cm^{-1} are illustrated in Fig. 4. In spite of the complexity of the present problem, the agreement between theory and experiment is excellent. The theory can thus be accepted with much confidence. Finally, two ''films'' showing molecular rotations are given in Fig. 5. The mean squared rotational angle $\sqrt{\langle\theta^2(\tau)\rangle}$ of the OH bond of HDO is illustrated as a function of time τ. The OH···O bond length is kept constant and equal to 2.99 A in curve (a), whereas it contracts from 2.99 A to 2.86 A in curve (b). One notices that rotational angles of the order of 35° are attained in times of the order of 700 fs. As a bending of this magnitude leads to a breaking of

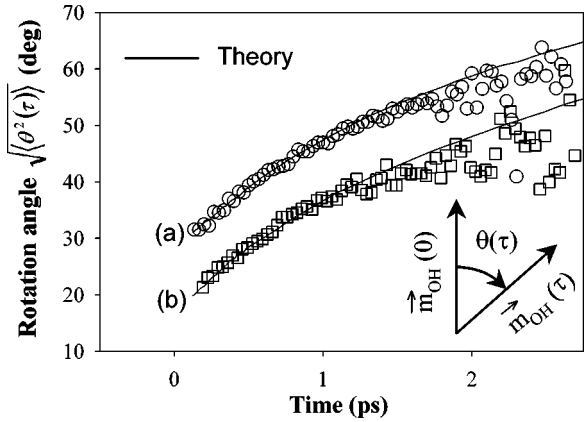

FIG. 5. Real time ''filming'' of HDO rotations. The measured quantity is the mean squared rotation angle $\sqrt{\langle\theta^2(\tau)\rangle}$ of the OH bond of HDO at time τ, starting from the initial OH bond direction; this angle is measured in degrees. The OH···O bond length is equal to 2.99 A in the curve (a), whereas it contracts from 2.99 A to 2.86 A in the curve (b). As expected, the OH rotations are slower in short OH···O bonds.

hydrogen bonds, one concludes that their lifetime in water is rotation limited. Unfortunately, our camera is blind at very short times where the pump and probe interact coherently: no ''filming'' is possible at those time scales. Note however that $\sqrt{\langle\theta^2(0)\rangle}$ is larger than zero for any finite pump and probe pulse duration. It is thus possible to ''film'' the HDO rotations in HDO/D_2O solutions. Not only the OH···O stretching motions but also the HDO rotations can be monitored by ultra-fast laser spectroscopy. Here again, the original Zewail approach proves extremely useful in visualizing molecular motions.

VI. DISCUSSION

Only a limited number of papers have yet been published concerning the coupling between molecular rotations and OH···O motions. In fact, the discovery of this subtle effect is recent[5–7] and its analysis remains partial. The following points merit attention. (i) The theory was first elaborated in a semiempirical form. A model was proposed in which the reorientation time is supposed to depend on frequency and in which the spectral diffusion is incorporated. Formulated in this way, the model was able to confirm that water molecules rotate in fact slower in short hydrogen bonds than in long ones. The activation energy of molecular reorientations was also derived.[6] However, the notion of an r-dependent rotational relaxation time τ_O remains to be precised. (ii) The possibility of monitoring rotational angles $\theta(\tau)$ as a function of τ has been also envisaged in classical infrared and Raman spectroscopy. However, their band shapes depend on rotational and on vibrational dynamics, simultaneously. The two types of motion must thus be disentangled from each other, if rotations are to be studied. This is usually done by employing the so-called VV−VH separation technique.[16] Rotational self-correlation functions obtained in this way are $\langle P_1(\cos(\theta(\tau)))\rangle$ for infrared and $\langle P_2(\cos(\theta(\tau)))\rangle$ for Raman; the latter is exactly the same as in pump−probe experiments. Rotational angles $\theta(\tau)$ can thus be, and have occasionally been, determined by employing the two classical techniques. Of course, the OH···O bond length selection is impossible in this case. For further reading, see Ref. 35. (iii) Molecular dynamics simulations of $\langle P_1(\cos(\theta(\tau)))\rangle$ and $\langle P_2(\cos(\theta(\tau)))\rangle$ showed that these functions exhibit a bump at time scales of the order of 100 fs; it was attributed to librational dynamics of water molecules; see Refs. 27 and 31 and many others. Unfortunately, this interesting feature is undetectable by the present technique. The present discussion may be closed by emphasizing the importance in the present context of short time domains below 200 fs. Normalizing the anisotropy to 2/5 at zero time propagates experimental errors to the rest of the spectrum and should be avoided.

ACKNOWLEDGMENTS

The authors gratefully acknowledge the support of the GDR 1017 of the CNRS during this work. The Laboratoire d'Optique et Biosciences is a Unité Mixte de Recherche No. 7645 of the CNRS and the Laboratoire de Physique Théorique des Liquides is a Unité Mixte de Recherche No. 7600 of the CNRS.

[1] G. Gale, G. Gallot, F. Hache, N. Lascoux, S. Bratos, and J-Cl. Leicknam, Phys. Rev. Lett. **82**, 1068 (1999).
[2] S. Bratos, G. Gale, G. Gallot, F. Hache, N. Lascoux, and J-Cl. Leicknam, Phys. Rev. E **61**, 5211 (2000).
[3] M. Dantus, M. Rosker, and A. H. Zewail, J. Chem. Phys. **87**, 2395 (1987).
[4] R. Bernstein and A. H. Zewail, J. Chem. Phys. **90**, 829 (1989).
[5] S. Woutersen, U. Emmerichs, and H. Bakker, Science **278**, 658 (1997).
[6] H. K. Nienhuys, R. V. Santen, and H. Bakker, J. Chem. Phys. **112**, 8487 (2000).
[7] H. Bakker, S. Woutersen, and H. K. Nienhuys, Chem. Phys. **258**, 233 (2000).
[8] H. Graener, G. Seifert, and A. Laubereau, Phys. Rev. Lett. **66**, 2092 (1991).
[9] R. Laenen, C. Rauscher, and A. Laubereau, Phys. Rev. Lett. **80**, 2622 (1998).
[10] R. Laenen, C. Rauscher, and A. Laubereau, J. Phys. Chem. B **102**, 9304 (1998).
[11] J. Stenger, D. Madsen, P. Hamm, E. T. J. Nibbering, and Th. Elsaesser, Phys. Rev. Lett. **87**, 027401 (2001).
[12] W. Mikenda, J. Mol. Struct. **147**, 1 (1986).
[13] T. Tao, Biopolymers **8**, 609 (1969).
[14] G. Fleming, J. Morris, and G. Robinson, Chem. Phys. **17**, 91 (1976).
[15] A. Tokmakoff, J. Chem. Phys. **105**, 1 (1996).
[16] S. Bratos and E. Maréchal, Phys. Rev. A **4**, 1078 (1971).
[17] J. S. Baskin, M. Chachisvilis, M. Gupta, and A. H. Zewail, J. Phys. Chem. **102**, 4158 (1998).
[18] S. Bratos and J-Cl. Leicknam, J. Chim. Phys. Phys.-Chim. Biol. **93**, 1737 (1996).
[19] S. Bratos and J-Cl. Leicknam, J. Chem. Phys. **109**, 9950 (1998).
[20] H. K. Nienhuys, S. Woutersen, R. V. Santen, and H. Bakker, J. Chem. Phys. **111**, 1494 (1999).
[21] S. Woutersen and H. J. Bakker, Phys. Rev. Lett. **83**, 2077 (1999).
[22] M. Diraison, Y. Guissani, J-Cl. Leicknam, and S. Bratos, Chem. Phys. Lett. **258**, 348 (1996).
[23] A. Geiger, P. Mausbach, J. Schnitker, R. L. Blumberg, and H. Stanley, J. Phys. (France) **45**, C7 (1984).
[24] J. Marti, J. Padro, and E. Guardia, J. Chem. Phys. **105**, 639 (1996).
[25] A. Luzar and D. Chandler, Nature (London) **379**, 55 (1996).
[26] M. Nakahara, in *Physical Chemistry of Aqueous Solutions*, edited by H. White, J. Sengers, D. Neumann, and J. Bellows (Begell House, New York, 1995), p. 449.
[27] R. Impey, P. Madden, and I. McDonald, Mol. Phys. **46**, 513 (1982).

[28] H. Berendsen, J. Grigera, and T. Straatsma, J. Phys. Chem. **91**, 6269 (1992).
[29] K. Watanabe and M. Klein, Chem. Phys. **131**, 157 (1989).
[30] D. V. Belle, M. G. Froeyen, G. Lippens, and S. Wodak, Mol. Phys. **77**, 239 (1992).
[31] I. Svishchev and P. Kusalik, J. Phys. Chem. **98**, 728 (1994).
[32] S. Mukamel, *Principles of Nonlinear Optical Spectroscopy* (Oxford University Press, New York, 1995).
[33] G. Tarjus and S. Bratos, Phys. Rev. A **30**, 1087 (1984).
[34] S. Bratos and J-Cl. Leicknam, J. Chem. Phys. **101**, 4536 (1994).
[35] W. C. Rothschild, *Dynamics of Molecular Liquids* (Wiley, New York, 1984), p. 135.